Understanding Shunting Mechanisms in Silicon Cells: A Review

O. Breitenstein
Max Planck Institute of Microstructure Physics, Halle
Weinberg 2, D-06120 Halle (Saale), Germany
phone: +49 345 5582740, electronic mail: breiten@mpi-halle.mpg.de

Lock-in thermography (LIT) is until now the most successful technique for imaging local inhomogeneities of the dark forward and reverse current in solar cells and thus for investigating shunts in solar cells. By combining LIT and other microscopic investigations, meanwhile many different shunt mechanisms have been identified in silicon solar cells, which may show either a linear (ohmic) or a non-linear (diode-like) I-V characteristic. In addition, there is a third type of "shunts" having a great importance for the reliability of modules, which are pre-breakdown sites. While pre-breakdown sites are only little investigated yet, the physical nature of the most common linear and non-linear shunts in silicon cells is quite well understood now. Ohmic shunting may be due to (1) incomplete opening of the edge, (2) alloyed-in Al-particles or other metals at the surface, (3) cracks before processing, and (4) highly n-conducting silicon carbide filaments crossing the cell (only in multicrystalline cells). Non-linear (diode-like) shunts are (1) due to a direct contact of the grid metal to the base (Schottky-type) or (2) due to highly recombinative locally extended defects crossing the pn-junction (recombination-type). These defects may be material-induced (grain boundaries, dislocations, precipitates) or process-induced, like, e.g., a non-passivated edge region of the cell or scratches or fresh cracks. These local recombination shunts, rather than the material properties, are dominating the recombination of most solar cells. For a high local density of states in these defects, the recombination current shows an ideality factor larger than 2. Here the recombination occurs no longer via isolated point defect states but via multi-level recombination, which may show intrinsic saturation effects.

1. Introduction

Traditionally the name "shunts" was used only for ohmic connections between n- and p-side of pn junctions, like an incompletely opened emitter at the edge. Generally, shunts are leading to leakage currents in solar cells, thereby reducing their fill factor (FF) and the open circuit voltage (V_{oc}) in operation, but not the short circuit current I_{sc}. However, already early shunt investigations have shown that there are both shunts showing a linear (ohmic) I-V characteristic and showing a non-linear (diode-like) characteristic [1]. Therefore, in the following we will use an extended definition of "shunts" as all local sites in solar cells where the local current significantly exceeds the homogeneously flowing current. With other words, our definition of "shunts" includes all sites of the cell which cannot be described by a 1-dimensional (e.g. PC1D) model, which assumes a homogeneous cell made from homogeneous semiconductor material. We will see that, besides obvious ohmic shunts like an incompletely opened edge, all kinds of shunts are connected with extended crystal defects, which are not included in a 1-dimensional solar cell model. This definition includes, besides ohmic shunts, also non-linear shunts including edge currents and pre-breakdown sites.

At the beginning of solar cell technology, only the measured parallel resistance (R_p) was an indication about the presence of shunts. Later on steady-state infrared thermography was used to image shunts [2]. However, the sensitivity of even modern thermocameras is not sufficient to image

weaker shunts under forward bias close to the maximum power point, which is in the order of 0.5 V. Instead, a reverse bias of -5 to -10 V had to be applied to the cells to image the shunts thermally [2]. Another problem of direct thermography was the high heat conductivity of silicon, which leads to a very blurred appearance of the thermograms, thereby reducing the effective spatial resolution. The same limitations hold for liquid crystal sheet shunt detection [3]. The understanding of shunts in solar cells has very much improved after the introduction of lock-in thermography (LIT) techniques [4], which, due to their dramatically improved sensitivity, for the first time allowed for imaging shunts also under forward bias of the cell, corresponding to normal operating conditions. Moreover, due to the dynamic nature of this measurement technique, lateral heat diffusion is suppressed, leading to a considerably improved effective spatial resolution. Recently, also electroluminescence (EL) and photoluminescence (PL) techniques have been found to be effective in shunt detection [5, 6].

Localizing shunts is only the first step in understanding them, the next step must be to identify their nature in order to avoid them. This has been done extensively by microscopic and microanalytical techniques, including visible light microscopy, near infrared transmission light microscopy, transmission electron microscopy (TEM), and scanning electron microscopy (SEM) in secondary electron (SE), electron beam-induced current (EBIC), and energy-dispersive X-ray analysis (EDX) mode. In the following, after a brief summary over existing shunt detection techniques, an overview is given about the most important shunt mechanisms in silicon cells, which have been identified hitherto. Finally, the recombination mechanism of non-linear recombination-induced shunts is discussed in more detail. It is found that recombination via extended defects showing a high local density of recombination states may lead to inherent saturation effects, which is the key for understanding the commonly measured large ideality factors of the recombination current of solar cells.

2. Shunt detection techniques

The most simple and cheapest technique for shunt detection, which is also widely used now in research and industry, is the liquid crystal (LC) sheet technique [3, 7]. About 160 µm thick plastic sheets, which are containing a thermochromic LC layer film, are available e.g. from EdmundOptics. The most appropriate type is No. 72-374 being sensitive between 25 and 30°C (77 - 86°F). Such a sheet is sucked to or simply laid on top of the cell to be investigated, and a reverse bias of several Volts is applied to the cell. In the position of ohmic shunts or pre-breakdown sites, the temperature rises and the color of the sheet changes from black via brown and green to blue. The limitations of this technique are the following: (1) Due to the thickness of the sheets and due to the lateral heat diffusion in silicon, the accuracy of localization is only in the order of 1 mm. (2) The sensitivity of this technique is so low that it can be used only under reverse bias, which may be as large as many Volts. Hence, non-linear shunts, which are active only under low forward bias, cannot be detected by the LC sheet technique if they are not also pre-breakdown sites. The blurring influence of the lateral heat conduction in the silicon can be reduced by sucking the cells to a massive copper chuck. Then the heat diffuses mainly vertically from the cell into the heat sink, and lateral heat diffusion is suppressed on cost of a reduced sensitivity.

Steady-state thermography is only rarely used for shunt detection in silicon cells, since it shows the same limitations as LC sheet imaging. The breakthrough in shunt analysis came with the application of lock-in thermography (LIT) techniques. LIT means that the power dissipation in a device is periodically modulated (usually on/off square-pulsed with a frequency between 1 and 100 Hz), and the measured surface temperature data are evaluated and summed up over many periods to yield an image of the local temperature modulation amplitude and of the local phase shift between heat dissipation and temperature modulation [4]. LIT by using an infrared (IR) thermocamera and

on-line data processing was introduced in 1988 for failure analysis in electronic components [8]. In the 1990s this technique became popular for non-destructive evaluation (NDE) of materials, hence for detecting sub-surface defects in solid bodies, and for local stress analysis [9]. The first LIT application to solar cells was made in 1994 by using "Dynamic Precision Contact Thermography" (DPCT) [1]. This technique, which used an x-y-z table to sequentially scan a miniature thermistor across the surface in contact mode, delivered the first meaningful shunt images under forward bias. However, it was too slow for general use. In 2000, LIT based on an IR camera and on-line data processing was used for the first time for shunt imaging in solar cells [10]. While LIT systems dedicated to NDE and stress analysis are available since many years (e.g. by Cedip, Stress Photonics, e/de/vis), meanwhile also systems dedicated to solar cell analysis are commercially available (e.g. by Thermosensorik, Aescusoft, InfraTec).

The original operation mode of LIT, which is still the most successful one for shunt investigation, is LIT performed in the dark by applying a pulsed bias to the device (Dark Lock-in Thermography, DLIT) [4]. Here the cell must be electrically contacted, hence only readily processed cells can be investigated. The advantage of this technique is that the thermal signal is caused only by the currents flowing in the dark. Hence, with DLIT shunt currents can easily be quantified [11]. Recently several new LIT techniques have been introduced, which are using pulsed light irradiation instead of a pulsed bias [12, 13]. The advantage of these "illuminated Lock-in Thermography" (ILIT) techniques is that, in simplest case, they don't need an electrical contact to the cell, hence they can image shunts already in an early technological state of processing. If there is a contact to the cells, depending on the electric load of the cell, different ILIT operation modes are possible, which are leading to different physical meanings of the obtained images (V_{oc}-ILIT, J_{sc}-ILIT, mpp-ILIT) [14]. A special technique called R_s-ILIT is able to image local inhomogeneities of the series resistance [15]. The limitation of all ILIT techniques (except R_s-ILIT) is that here the heat generation includes also carrier thermalization heat, both in the base and at the pn-junction, which leads to a homogeneous background signal and complicates the quantitative evaluation of the results [16].

Recently also electroluminescence (EL) and photoluminescence (PL) techniques have been proposed for shunt imaging [5, 6]. The resulting images are looking very similar to Light Beam-Induced Current (LBIC) images, but here the shunt imaging effect relies on the local reduction of the intrinsic bias around the shunts. A recent comparison between PL, EL, and DLIT has shown that stronger ohmic shunts and also some pre-breakdown sites can be imaged reliably by luminescence techniques, but weaker ohmic and non-linear shunts can not [17].

3. Shunt types

3.1. Pre-breakdown sites

Pure pre-breakdown sites show a low conductivity under low forward and reverse bias, but an exponentially increasing one at higher reverse bias. Hence, they do not decrease the parallel resistance R_p. Since they may create hot spots in a module by shading some cells, whereby the shaded cell may come under higher reverse bias, they may be dangerous for the reliability of solar modules [18]. Regarding a base doping concentration of 10^{16} cm^{-3}, solar cells should stand a reverse bias of nearly -100 V. In reality, especially multicrystalline (MC) cells often start to break down already between -5 and -15 V. Very little is known until now about the nature of pre-breakdown sites. Several authors have observed visible and IR light emission at pre-breakdown sites and have concluded that this is due to some avalanche effect [19]. So the reason for the pre-breakdown sites should be a local increase of the electric field in the junction region due to a non-planar shape of the junction. Indeed, we have found pre-breakdown sites in a region containing voids in the material, which should lead to high local fields. Similar effects are expected in positions where the pn-junction is spiking, e.g. at certain grain boundaries with preferential P diffusion. Fig. 1 shows a reverse bias

DLIT image of a pre-breakdown site (a) and a SEM image of a polished surface (b) of the shunt region where the voids are visible. This has been a pure pre-breakdown site, hence at low forward and reverse voltage there was no shunt in this region. Another example of pre-breakdown sites is shown in Fig. 2 [17]. Here the left image (a) shows DLIT results and the right image a luminescence image, both measured at -5 to -6 V reverse bias. The insets show that here the breakdown sites are below grid lines. Maybe in these sites there is a direct contact between grid lines and base material, yielding a kind of Schottky contact, which breaks down at relatively low reverse bias. Another explanation is that here some metallic impurities have diffused from the grid material to the pn-junction, leading to an increased generation current there, which is avalanche-multiplied under reverse bias. This interpretation is supported by the fact that in many cases pre-breakdown sites have been seen in positions of non-linear shunts (see section 3.3). Obviously, if there is a recombination-active defect crossing the pn-junction, which leads to a recombination current under low forward bias, this defect also leads to a generation current under low reverse bias. Under low reverse bias this generation current is so low that it remains undetectable by DLIT, but at higher reverse bias this generation current is amplified by avalanche multiplication, then leading to the typical pre-breakdown sites. This hypothesis, however, still has to be proven. To summarize, until now there is evidence for three mechanisms for pre-breakdown sites: (1) High field strengths due to a non-planar pn-junction, (2) breakdown of a Schottky-type shunt, and probably (3) avalanche amplification of the generation current of an extended defect crossing the pn junction.

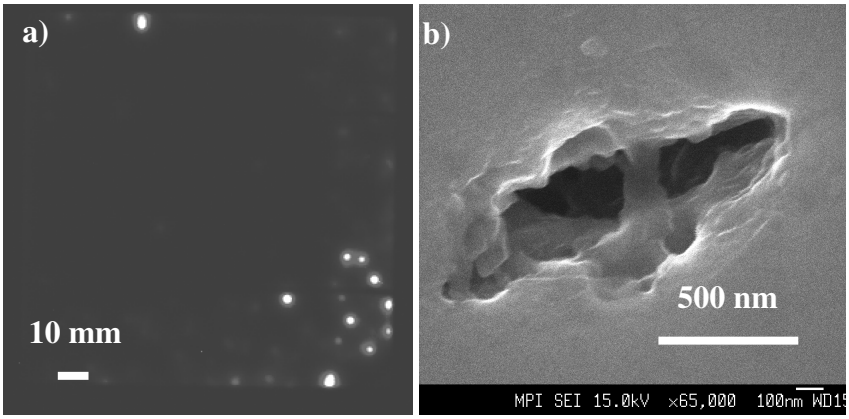

Fig. 1: DLIT image of a MC cell taken at -12 V reverse bias (a), and SEM (SE) image of a void in a pre-breakdown position after polishing the surface

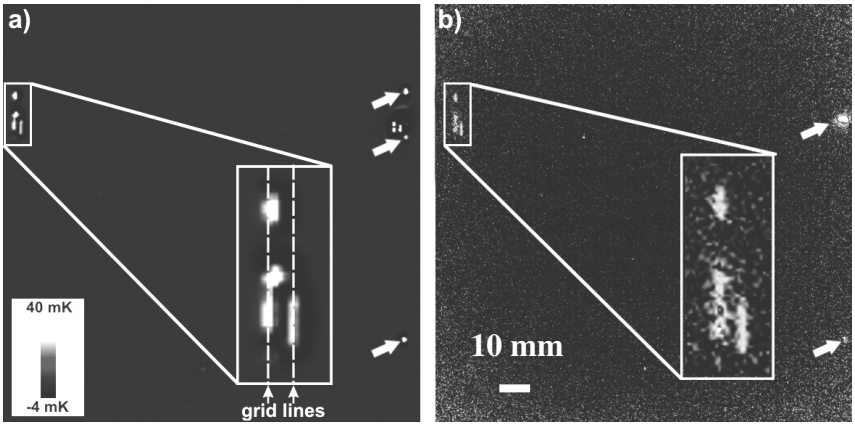

Fig. 2: DLIT image taken at -6 V (a) and electroluminescence (EL) image taken at -5 V (b) of a MC cell. The arrows at the right are pointing to some point-like pre-breakdown sites, which are only partly visible in EL [17]

3.2. Linear (ohmic) shunts

Only this type of shunts is significantly reducing the parallel resistance R_p of the cell. Linear shunts can easily be recognized by the fact that in the DLIT amplitude image they show the same brightness (= temperature modulation amplitude) at + 0.5 V forward bias and -0.5 V reverse bias. Since the dissipated power increases for linear shunts with the square of the applied bias, they can easily be detected under higher reverse bias by LC sheet imaging. The most trivial case of a linear

shunt is an incompletely opened edge of a cell, which shows up in DLIT as a bright spot or line at the edge [1]. The residual emitter at the edge can nicely be imaged by SEM (EBIC) [20]. A similar mechanism holds if a cracked wafer is processed. Also then the emitter may go through the crack up to the back contact, thereby creating a linear shunt. During screen printing of contacts even metal paste may be squeezed through a crack, after firing creating a very strong ohmic shunt [20]. Another important linear shunt type is created by Al particles at the surface, which may come e.g. from stacking solar cells after drying and before firing the metal pastes. If such an Al particle is lying on top of a solar cell, during a subsequent firing step it alloys into the surface, creating a p^+-region around. This p^+-region is in direct (ohmic) contact to the p-base, and it yields a tunnel-junction to the surrounding n^+-emitter, thereby producing an ohmic connection between emitter and base [20]. Fig. 3 shows a SEM (SE) image of an Al particle on the surface of a monocrystalline solar cell together with an EDX spectrum showing the Al lines. Not only Al creates ohmic shunts if it is alloyed into the emitter. Fig. 4 shows a region in a solar cell where the surface was cut by a Nd:YAG laser [21]. Where the grid lines were cut by the laser, (nearly) ohmic shunts appear. Obviously the grid line material contains certain impurities (Al, B?), which are creating ohmic shunts if they are alloyed into the emitter, either due to p^+ doping or due to the introduction of a very high density of gap states. Outside of the grid line positions, the Nd:YAG laser generates only non-linear shunts (see section 3.4.). The laser parameters can be selected in such a way that the creation of ohmic shunts can be avoided [21].

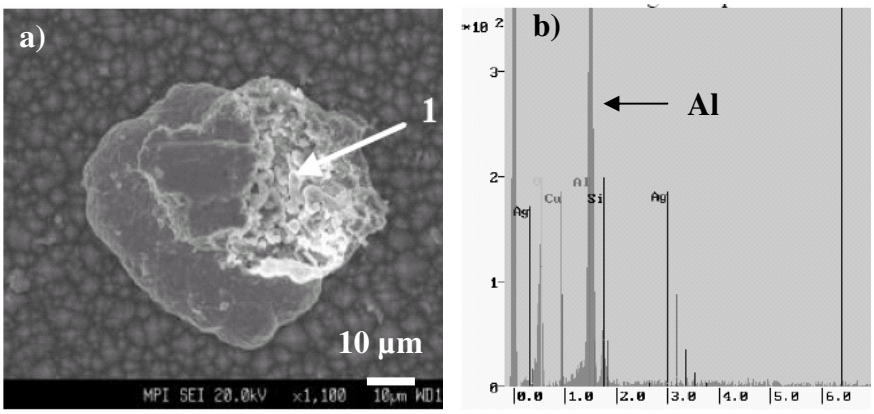

Fig. 3: SEM (SE) image (a) and EDX spectrum of an Al particle on top of a solar cell, which created an ohmic shunt

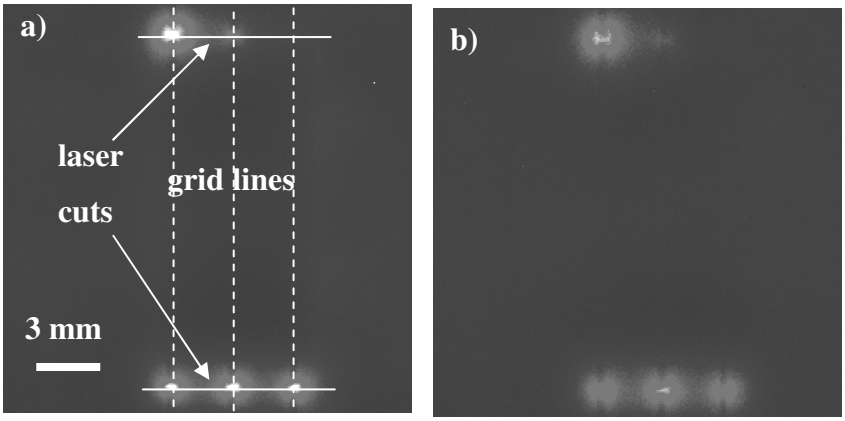

Fig. 4: Forward bias (a) and reverse bias (b) DLIT image of a region cut with a Nd:YAG laser [21]

Another important ohmic shunt type exists only in multicrystalline (MC) material. Especially in the uppermost part of the silicon block there may be a supersaturation of dissolved carbon (C) in the Si melt. This C tends to precipitate during the cooling phase in the block in form of SiC filaments, which are growing preferentially in large-angle grain boundaries. By performing microscopic 4-probe measurements including conductivity type detection on single SiC filaments, we have found

that they are highly n-conducting [22]. The doping is most probably due to N, which also exists in the melt, since the crucibles are covered by a Si_3N_4 layer. By performing EBIC on the polished backside of a solar cell containing such shunts, we have proven that these shunts are yielding n-conducting channels crossing the whole bulk of the cell [20, 22]. These channels are directly electrically connected to the emitter, and they may also be electrically connected to the base contact, either by direct contact to the base contact metal (Al) or by yielding a tunnel junction to the p^+ BSF layer. However, we have found that not all SiC filaments crossing the cell are making ohmic shunts. Until now it is not clear under which conditions the SiC filaments are making ohmic shunts. Fig. 5 shows an EBIC image of the backside of a cell, showing the n-conducting channels along a grain boundary, and the corresponding SE image of a lightly etched backside of a shunt region in a MC cell. The bright spots in the EBIC image are the n-conducting channels crossing the whole cell.

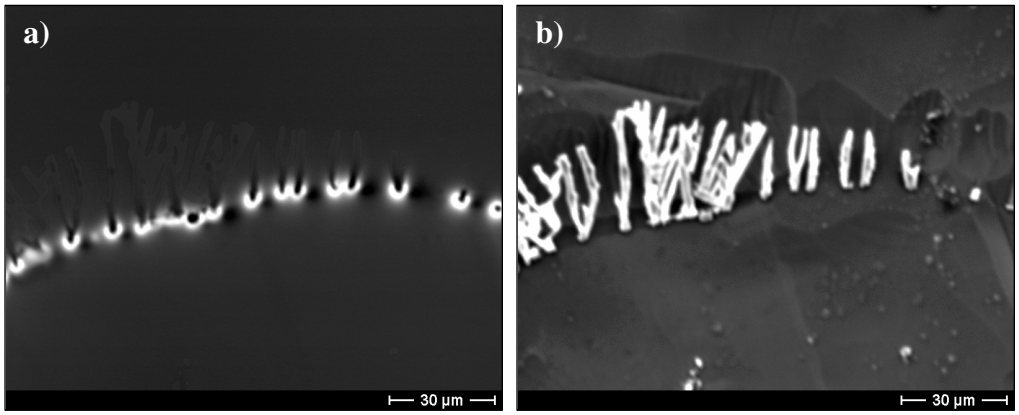

Fig. 5: EBIC image (a) and SE image (b) of a linear shunt region, taken from the lightly etched backside of the cell

To summarize, altogether 5 mechanisms creating linear (ohmic) shunts were found: (1) Incompletely opened emitter at the edge, (2) crack, containing an emitter layer or metal paste, (3) Al particle at the surface, (4) laser cut through a grid line, and (5) SiC filaments in MC material.

3.3. Schottky-type shunts

It had already been mentioned in section 3.1. that, due to an unusually thin emitter layer or to inappropriate grid firing conditions, the grid metal of the emitter may come in contact with the base material. Another mechanism for Schottky-type shunts has been described in [20], which are texturization tips, which are mechanically truncated after emitter formation, thereby exposing the bare base material to the surface. There may be also other reasons leading to a "hole" in the emitter layer, e.g. dust particles at the surface during emitter formation or scratches after emitter diffusion. If the emitter grid crosses such a site, the grid metal comes in direct contact to the base. It can be expected that such a "Schottky junction" is everything else but an ideal Schottky diode. Only for ideal Schottky diodes we expect an ideality factor of 1 of the I-V characteristic. Note that forming ideal Schottky diodes requires extremely pure metallization conditions, which are definitely not given here. Instead, we expect the formation of a "dirty" Schottky diode implying certain interface layers, which govern its electric properties. It is well-known that "dirty" Schottky diodes may show a recombination factor larger than 1 and even larger than 2 [23]. Nevertheless, they show a certain rectifying characteristic and also pre-breakdown behavior. Hence, their I-V characteristic is non-linear (diode-like) with preferred conduction under forward bias of the cell. Indeed, Huster et al. [24] have shown that intentionally made Schottky shunts show a combination of rectifying and ohmic behavior. This makes Schottky-type shunts electrically similar to recombination-induced non-linear shunts, which are described in the following section. In fact, if a non-linear shunt or a pre-breakdown site is in the position of a grid line (see Fig. 2), it can only be suspected that this is a Schottky-type shunt. An alternative explanation of such a shunt would be that the underlying Si

material is "poisoned" by certain impurities coming from the grid metal paste. A clear distinction between Schottky-type and recombination-induced shunts could only be made e.g. by high-resolution EBIC imaging of the underlying n^+-layer and its separate pn-junction in cross section. To the knowledge of the author, such an investigation has never been performed yet.

3.4. Recombination-induced shunts

According to the well-known two-diode model of a solar cell, there are two exponential components of the dark forward current: (1) The diffusion current (described by I_{01}) showing an ideality factor of $n_1 = 1$, and (2) the recombination current (described by I_{02}) showing an ideality factor of $n_2 \leq 2$. While the diffusion current is essentially due to electron injection from the emitter into the base, the recombination current is due to recombination in the depletion region. It has been found by several authors that, in absence of other shunts (in monocrystalline material), I_{02} is not proportional to the area but to the circumference of a cell. Obviously here the non-passivated edge represents a local (2-dimensional) extended defect crossing the pn-junction, which dominates I_{02} of the whole cell. Indeed, this edge leakage current can be imaged by DLIT under forward bias, as shown in Fig. 6. This sample was a MC cell with laser-isolated edges, where the left part was broken off. The original edges (at the top, right, and bottom) clearly show a higher leakage current (bright line) under forward bias than the broken edge at the left. Moreover, there are two ohmic shunts at the top (appearing also under reverse bias) and a lot of other shunts in the area, which also appear only under forward bias. These are typical material-induced non-linear shunts, which are caused by recombination-active extended crystal defects like dislocations, grain boundaries, or precipitates (see [20]), or by local material pollutions. Also scratches at the surface or fresh cracks of the cell are leading to non-linear recombination-induced shunts [20]. In fact, for most crystalline solar cells, the recombination current I_{02}, which dominates at + 0.5V forward bias, is not governed by the lifetime in the material, as predicted by elementary diode theory, but is mostly due to local extended crystal defects crossing the pn-junction. In the absence of material-originated recombination-active local defects, the usually non-passivated edge is the dominating recombination-induced "shunt". Only if the edge is lying well-passivated below a thermal oxide, as it is common for very high quality solar cells like PERL or PERT cells, the influence of the edge current or other recombination-induced shunts to I_{02} may be negligible.

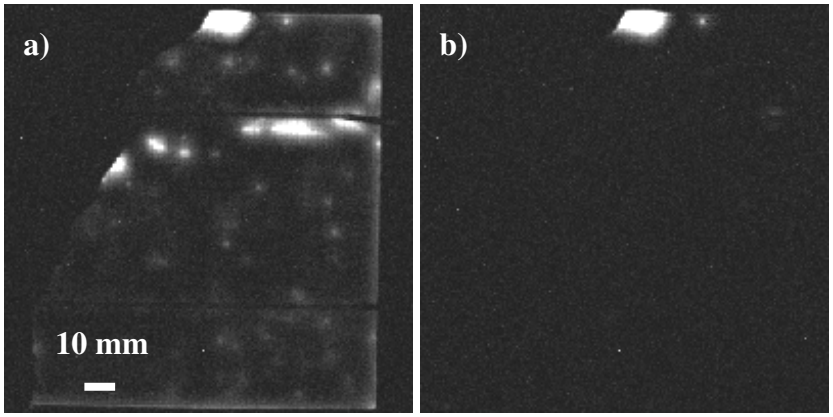

Fig. 6: DLIT image of a part of a MC solar cell, which was laser edge-isolated, measured under +0.5 V forward bias (a) and -0.5 V reverse bias (b)

4. Understanding ideality factors larger than two of the dark I-V characteristic

According to the Shockley-Read-Hall (SRH) recombination model assuming isolated point defects, the ideality factor of the recombination current n_2 should be 2 or below. However, in many cases large values of $n_2 = 3$ or above have been measured [25]. Moreover, the quantitative value of I_{02} is usually several orders of magnitude larger than expected for the given lifetime in the base material [26]. Finally, in contrast to the saturation-type reverse characteristic expected by standard

diode theory, the reverse characteristic of most solar cells is linear or even superlinear. All these deviations from classical diode theory can be explained by the fact that I_{02} is not due to homogeneously distributed point defects but to local extended defects crossing the depletion region, as it has been shown in the previous section. Ideality factor mapping, which can also be done by performing DLIT at two different forward biases [11], indeed has revealed that also in MC cells the biggest part of the area shows an ideality factor close to 1, whereas all shunts, including the edge, show a large ideality factor, which may exceed 4. Nevertheless, for some cells with non-passivated edges $n_2 = 2$ holds. To clarify this obviously different behavior, diamond scratches with different loads have been made at room temperature on PERT cells, which originally all showed an ideal I-V characteristic with an ideality factor < 1.5 over the whole bias range [27].

Fig. 7 shows the resulting bias-dependent ideality factors. Since the scratch was between two grid lines, the series resistance R_s to this "artificial shunt" was easy to calculate with the R_s-corrected results also given for the highest load in Fig. 7. We see that for the lowest load, where the scratch did not reach the pn-junction yet, the ideality factor increases but remains at or below 2, but for the highest loads it exceeds even 4 over a large bias range. Our interpretation is that for a low defect density the defects are still isolated, hence they behave according to the Shockley-Read-Hall (SRH) recombination model. If the local defect density drastically increases, since the scratch is cutting through the pn-junction, the SRH model is not applicable anymore, but multi-level recombination has to be considered. We have shown that already considering simple two-level pair recombination is sufficient to describe saturation effects, which may lead to ideality factors larger than 2 in a limited bias range [27]. However, a generally accepted theory for multi-level recombination is still missing.

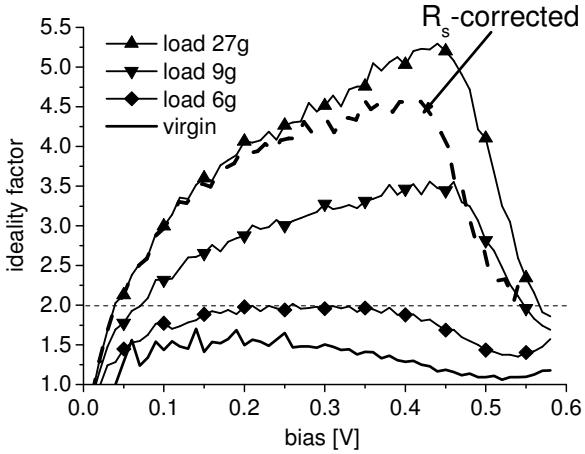

Fig. 7: Bias-dependent ideality factor of different PERT cells after diamond scratching under different loads. Dashed: 27 g results R_s-corrected.

Also the reverse characteristic of the scratched PERT cells drastically changed [27]. In the original cells the reverse current was in the low nA range and saturation-type, but it increased by several orders of magnitude and became linear in the scratched cells. Nevertheless, the current under -0.5 V reverse bias was still some orders of magnitude lower than the forward (recombination) current, so that it was not visible in DLIT (as for the non-linear shunts in Fig. 6). The temperature dependence of the reverse current was linear over $1/T^{1/4}$ in a wide temperature range, which is an indication of hopping conduction [28]. We believe that this is also a consequence of the high local density of states in the shunting defects, which allows inter-level transport across the pn-junction.

5. Conclusions

Since the introduction of lock-in thermography, the degree of understanding shunts in silicon solar cells has drastically improved. It is clear now that only certain shunt types have an ohmic characteristic, but many others have a non-linear one. Here one has to distinguish the behavior under low bias (+/- 0.5 V) from that under large reverse bias (several Volts), where pre-breakdown occurs. In this contribution we have identified two different pre-breakdown mechanisms, which are Schottky-type breakdown at grid lines and high local fields at a non-planar pn-junction, but certainly there are more mechanisms. Since pre-breakdown sites are often occurring in positions of non-linear

shunts, we are proposing here that also the generation current of extended defects crossing the pn-junction may get avalanche-multiplied under high reverse bias, but this hypothesis still has to be proven. Non-linear shunts at low bias may be due to Schottky-type defects (direct contact of grid lines to the base) or may be recombination-type shunts. The latter are caused by locally extended defects crossing the pn-junction. These may be the unpassivated edge of the cell, grown-in recombination-active crystal defects like dislocations, grain boundaries, or precipitates, or technological faults like scratches or fresh cracks. Ohmic shunts are due to an incompletely opened emitter layer at the edge, cracks containing an emitter layer or metal paste, Al particles at the surface, laser cuts through a grid line, or SiC filaments in MC material. The non-ideal I-V characteristic of most commercial solar cells, consisting in an unexpectedly large recombination current with a large ideality factor and an ohmic or superlinear reverse characteristic, can completely be explained by the fact that both the recombination current under forward bias and the reverse current are dominated by local extended defects, leading to non-linear shunts. An essential contribution to this current, both for mono- and multicrystalline cells, is the unpassivated edge region. Depending on the local density of recombination states in these defects, the recombination current may show either an ideality factor of $n_2 = 2$ or below, as predicted by SRH theory, or a higher n_2 due to the increasing dominance of multi-level recombination. Also a linear or superlinear reverse characteristic can be explained by hopping conduction across shunting extended defects with a high density of states.

The author is indebted to many colleagues and companies for fruitful cooperation in the last years, especially to I. Konovalov (now Leipzig), M. Langenkamp (now Rendsburg), J.P. Rakotoniaina (now Berlin), M.H. Al Rifai (now Dresden), P. Altermatt and K. Ramspeck (Hameln), A. Schenk (Zürich), St. Glunz and W. Warta (Freiburg), G. Hahn and M. Kaes (Konstanz), M.A. Green, M.D. Abbott, R.A. Bardos, and T. Trupke (Sydney), and to J. Bauer, R. Gupta, H. Leipner, and M. Werner (Halle), as well as to the companies Thermosensorik (Erlangen), Q-Cells (Thalheim), Photowatt (Bouroin-Jallieu), Deutsche Cell (Freiberg), Sunways (Arnstadt), and BP (Tres Cantos). This work was supported by BMU projects ASIS (0329846D) and SolarFocus (0327650D).

References

[1] O. Breitenstein, W. Eberhardt, K. Iwig, Imaging the Local Forward Current Density of Solar Cells by Dynamical Precision Contact Thermography, Proc. 1st WCPEC, Hawaii 1994, pp. 1633-1636

[2] A. Simo and S. Martinuzzi, Hot Spots and Heavily Dislocated Regions in Multicrystalline Silicon Cells, 21st IEEE PVSC, Kissimee 1990, pp. 800-805

[3] C. Ballif, S. Peters, J. Isenberg, S. Riepe, D. Borchert, Shunt Imaging in Solar Cells Using Low Cost Commercial Liquid Crystal Sheets, Proc. 29th IEEE PVSC, New Orleans 2002, pp. 446-449

[4] O. Breitenstein, M. Langenkamp, *Lock-in Thermography*, Springer 2003

[5] M. Kasemann, M.C. Schubert, M. The, M. Köber, M. Hermle, W. Warta, Comparison of Luminescence Imaging and Illuminated Lock-in Thermography on Silicon Solar Cells, Applied Physics Letters 2006, **89**: 224102, DOI: 10.1063/1.2399346

[6] K. Bothe, P. Pohl, J. Schmidt, T. Weber, P. Altermatt, B. Fischer, R. Brendel, Electro-luminescence imaging as an in-line characterization tool for solar cell production, Proc. 21st Eur. PVSEC, Dresden 2006, pp. 597-600

[7] O. Breitenstein, J.P. Rakotoniaina, Comparison of Shunt Imaging by Liquid Crystal Sheets and Lock-in Thermography, Proc. 12th Workshop on Crystalline Solar Cell Materials and Processes, Breckenridge, Colorado 2002, pp. 244-247

[8] P.K. Kuo, T. Ahmed, H. Jin, R.L. Thomas, Phase-Locked Image Acquisition in Thermography, SPIE **1004** (1988), 41
[9] X.P.V. Maldague, *Theory and Practice of Infrared Technology for Nondestructive Testing*, Wiley 2001
[10] O. Breitenstein, M. Langenkamp, O. Lang, and A. Schirrmacher, Shunts due to laser scribing of solar cells evaluated by highly sensitive lock-in thermography, Solar Energy Materials and Solar Cells **65** (2000), 55
[11] O. Breitenstein, J.P. Rakotoniaina, M.H. Al Rifai, Quantitative Evaluation of Shunts in Solar Cells by Lock-in Thermography, Prog. Photovolt: Res. Appl. **11** (2003), 515
[12] J. Isenberg, W. Warta, Realistic Evaluation of Power Losses in Solar Cells by Using Thermographic Methods, Journal of Applied Physics **95** (2004), 5200
[13] M. Kaes, S. Seren, T. Pernau, G. Hahn, Light-modulated Lock-in Thermography for Photosensitive pn-Structures and Solar Cells, Prog. Photovolt: Res. Appl. **12** (2004), 355
[14] O. Breitenstein, J.P. Rakotoniaina, G. Hahn, M. Kaes, T. Pernau, S. Seren, W. Warta, J. Isenberg, Lock-in Thermography – A Universal Tool for Local Analysis of Solar Cells, Proc. 20th Eur. PVSEC, Barcelona 2005, pp. 590-593
[15] O. Breitenstein, J.P. Rakotoniaina, A.S.H. van der Heide, J. Carstensen, Series Resistance Imaging in Solar Cells by Lock-in Thermography, Prog. Photovolt: Res. Appl. **13** (2005), 645
[16] O. Breitenstein, J.P. Rakotoniaina, Electrothermal simulation of a defect in a solar cell, J. Appl. Phys. **97** (2005), 074905
[17] O. Breitenstein, J. Bauer, T. Trupke, R.A. Bardos, On the detection of shunts in silicon solar cells by photo- and electroluminescence imaging, sent to Prog. Photovolt: Res. Appl.
[18] W. Herrmann, M.C. Alonso, W. Boehmer, K. Wambach, Effective hot-spot protection on PV modules – characteristics of crystalline silicon cells and consequences for cell production, Proc. 17th Eur. PVSEC, Munich 2001, pp. 1646-1649
[19] A.G. Chynoweth, K.G. McKay, Photon emission from avalanche breakdown in silicon, Physical Review **102** (1956), 369
[20] O. Breitenstein, J.P. Rakotoniaina, M.H. Al Rifai, M. Werner, Shunt Types in Crystalline Silicon Solar Cells, Prog. Photovolt: Res. Appl. **12** (2004), 529
[21] M. D. Abbott, T. Trupke, H. P. Hartmann, R. Gupta and O. Breitenstein, Laser Isolation of Shunted Regions in Industrial Solar Cells, sent to Prog. Photovolt: Res. Appl.
[22] J. Bauer, O. Breitenstein, and J.P. Rakotoniaina, Electronic activity of SiC precipitates in multicrystalline solar silicon, phys. stat. sol. (a) **204** (2007), 2190
[23] E.H. Rhoderick and R.H. Williams, *Metal-Semiconductor Contacts*, Clarendon 1988
[24] F. Huster, S. Seren, G. Schubert, M. Kaes, G. Hahn, O. Breitenstein, P.P. Altermatt, Shunts in Silicon Solar Cells below Screen-Printed Silver Contacts, Proc. 19th Eur. PVSEC, Paris 2004, pp. 832-835
[25] A. Kaminski, J.J. Marchand, H. El Omari, A. Laugier, Q.N. Le, D. Sarti, Conduction Processes in Silicon Solar Cells, Proc. 25th IEEE PVSC, Washington DC 1996, pp. 573-576
[26] K.R. McIntosh, *Lumps, Humps and Bumps: Three detrimental Effects in the Current-Voltage Curve of Silicon Solar Cells*, Ph.D. Thesis, UNSW (Sydney) 2001
[27] O. Breitenstein, P. Altermatt, K. Ramspeck, A. Schenk, The Origin of Ideality Factors N>2 of Shunts and Surfaces in the Dark I-V Curves of Si Solar Cells, Proc. 21st Eur. PVSEC, Dresden 2006, pp. 625-628
[28] F. Mott, *Metal-Insulator Transitions*, Taylor and Francis 1990